

# Surface characteristics of Ti-5Al-2.5Sn in electrical discharge machining using negative polarity of electrode

Md. Ashikur Rahman Khan<sup>1</sup> · M.M. Rahman<sup>2,3</sup>

Received: 29 August 2016 / Accepted: 9 January 2017  
© Springer-Verlag London 2017

**Abstract** A large number of parameters significantly affect the performance of electrical discharge machining (EDM) which is a non-conventional technique. The choice of the EDM parameters depends on workpiece-electrode material combination. So, the selection of parameters becomes intricate. This manuscript presents the surface characteristics of the machined surface in EDM on Ti-5Al-2.5Sn titanium alloy. The surface roughness and the microstructure of the machined surface are explored for different EDM parameters and electrode materials. Experimentation was accomplished using negative polarity of copper, copper-tungsten and graphite electrode. In this study, peak current, pulse-on time, pulse-off time and servo-voltage are taken into consideration as process variables. The surface roughness is greatly influenced by peak current and pulse-on time among the selected electrical parameters. Among the three electrodes, the copper electrode produces the lowest surface roughness whilst graphite electrode gives the highest surface roughness. The surface characteristics (crater, crack and globule) are distorted on account of discharge energy. In context of fine surface characteristics, the copper can become as first choice electrode materials.

**Keywords** Surface characteristics · Ti-5Al-2.5Sn · Negative polarity · Electrode materials · Discharge energy

## 1 Introduction

Nowadays, titanium is one of the most important metals in industry [1]. Titanium has found its niche in many industries owing to its unique characteristics which make it preferable to other materials such as aluminium, steels and super alloys. Titanium is an allotropic element; it exists in more than one crystallographic structure. There are different types of titanium alloys such as Ti-6Al-4V, Ti-6Al-6V-2Sn, Ti-15V-3Cr-3Al-3Sn, Ti-5Al-5V-5Mo-3Cr, Ti-3Al-2.5V, Ti-10V-2Fe-3Al and Ti-5Al-2.5Sn alloy. Among these titanium alloys, the most common titanium alloys is Ti-6Al-4V. Although Ti-6Al-4V alloy has several advantages and wide application, it has the drawback of toxicity due to the presence of vanadium (V) [2]. Besides, the other common used titanium alloys such as Ti-6Al-6V-2Sn, Ti-15V-3Cr-3Al-3Sn, Ti-5Al-5V-5Mo-3Cr, Ti-3Al-2.5V and Ti-10V-2Fe-3Al also retain the vanadium. On the other hand, Ti-5Al-2.5Sn is V-free titanium alloy. Accordingly, Ti-5Al-2.5Sn (Ti-5-2.5) titanium alloy is an appreciated and important titanium alloy because it is not toxic to the environment like other titanium alloys. Ti-5Al-2.5Sn alloy is used in airframes and jet engines due to its good weldability, stability and strength at elevated temperatures [3, 4]. Ti-5Al-2.5Sn is also used for manufacturing steam turbine blades, autoclaves and other process equipment vessels operating up to 480 °C, high-pressure cryogenic vessels, aircraft engines, compressor blades, missile fuel tanks and structural parts operating for short times up to 600 °C, airframe and jet-engine parts, welded stator assemblies and hollow compressor blades [5]. Titanium aluminides have begun to be used for automotive components, including race car engine valves and turbocharger

---

✉ Md. Ashikur Rahman Khan  
ashik.nstu@yahoo.com

<sup>1</sup> Department of Information and Communication Engineering, Noakhali Science and Technology University, Noakhali 3814, Bangladesh

<sup>2</sup> Faculty of Mechanical Engineering, Universiti Malaysia Pahang, 26600 Pekan, Pahang, Malaysia

<sup>3</sup> Automotive Engineering Centre, Universiti Malaysia Pahang, 26600 Pekan, Pahang, Malaysia

rotors [6]. Possible automotive applications of titanium include connecting rods, piston pins, valves, valve springs, valve spring seats, bucket tappets, brake pins, camshafts and crankshafts. In spite of the increased utility of titanium alloys, the capability to produce parts products with high productivity and superior quality becomes challenging [7, 8]. It accrued a key problem in machining using conventional techniques [9, 10]. However, it can be machined effectively by a non-conventional technique, electrical discharge machining (EDM).

In EDM, there are no standard technologies readily available for setting the machining parameters to achieve the desired machining performance of titanium alloys, especially Ti-5Al-2.5Sn. Any slight variations in one of the process parameters can affect the machining performance measures such as surface roughness and cutting rate [11].

A small number of research works on EDM of titanium alloys has been published. Most of these studies, which are being stated here, are carried out with regard to Ti-6Al-4V titanium alloy. Chen et al. [12] investigated the electrical discharge machining characteristics on Ti-6Al-4V material altering the dielectric fluid. They used copper as electrode material and considered discharge current and pulse-on time as process variables. The feasibility of using distilled water as a dielectric fluid was studied. The material removal mechanism of Ti-6Al-4V with distilled water as well as kerosene is also investigated. Hascalik and Caydas [13] studied the machining characteristics of Ti-6Al-4V using different electrodes, namely graphite, copper and aluminium. They took into consideration only two process parameters as discharge current and pulse-on time to explore the influence of EDM parameters on various aspects of the surface integrity of Ti-6Al-4V. Caydas and Hascalik [14] attempted to model electrode wear and recast layer thickness in machining of Ti-6Al-4V through response surface methodology. Pulse current, pulse-on time and pulse-off time were employed as process parameters and graphite was utilized as electrode material. They also analysed electrode wear of graphite electrode and white layer thickness of Ti-6Al-4V material. It was explored that pulse current is the most important factor effecting both electrode wear and recast layer thickness, whilst pulse-off time does not possess any significance on both responses. It is required to examine the impact of pulse-off time that has been carried out in the current study. Fonda et al. [15] investigated the effect of thermal and electrical properties of the workpiece material Ti-6Al-4V in electrical discharge machining using copper as electrode and duty factor as process material. They considered only one process parameter as duty factor and simply one electrode material, copper. Rao et al. [16] carried out the electrical discharge machining for Ti-6Al-4V, HE15, 15CDV6 and M-250 material. Current, voltage and machining time were selected as process parameters, and copper was used as electrode material in order to represent material removal rate. Likewise, Rao et al. [17] investigated the surface roughness of Ti-6Al-4V,

HE15, 15CDV6 and M-250 materials in EDM. They conducted the experimental work considering current and voltage as process parameters and copper as electrode material. The optimum value of current and voltage in terms of surface roughness was also determined. The influence of workpiece material and process parameters—current and voltage was investigated in both research works [16, 17]. It was found that the type of workpiece material was having the highest influence on material removal rate and surface roughness. On the other hand, Kao et al. [18] studied the process variables such as voltage, current, pulse-on time, pulse-off time and duty factor. Here, they employed copper electrode material for EDM on Ti-6Al-4V. They attempted to optimize the electrical discharge machining performance, surface roughness of Ti-6Al-4V, through Taguchi and Grey relational analysis. The machining performance characteristics were investigated for mild steel workpiece using copper as electrode [19]. In this work, experiment was performed taking into account only single parameter, discharge current. It was shown that as the current increases, the temperature between the electrode and workpiece increases resulting in more vaporization of workpiece material. Pawade and Banwait [20] reviewed the research works carried out in the development of die-sinking EDM within the past decades for the improvement of machining characteristics. They also proposed programmable logic controller (PLC)-based flexible machine controller to enhance the machining characteristics and to achieve high-level automation. Khan and Rahman [21] developed a regression equation based on response surface methodology for correlating the interactive and higher-order influences of machining parameters on surface finish of Titanium alloy Ti-6Al-4V. On the other hand, several research works with EDM process have been carried out to investigate the surface roughness of distinct materials namely, aluminium alloy-silicon carbide composite, stainless steels 316 L and 17-4 PH, nickel-based super alloy inconel 718, NiTi alloy, H11 steel, hot die steel H11, aluminium-multiwall carbon nanotube composites (AL-CNT) and precipitation hardening stainless steel PH17-4 ([22, 23, 24, 25, 26, 27, 28, 29]). Most of these work examined the effect of process parameters on surface roughness. Besides surface roughness, Reddy et al. [28] analysed the effect of peak current, pulse-on time and pulse-off time on surface hardness. Daneshmand et al. [30] examined the effect of input parameters on surface roughness to determine the minimal surface roughness and maximal material removal of NiTi alloy. On the other hand, Pawade and Banwait [20] suggested flexible machine controller for die-sinking EDM to enhance the machining characteristics and to achieve high-level automation. Analytical dependence was established between the discharge energy parameters and the heat source characteristics [31]. In addition, the thermal properties of the discharged energy were experimentally investigated and their influence on surface roughness was established.

The literature review shows that the study with regard to surface characteristics in EDM on Ti-5Al-2.5Sn titanium alloy for distinct electrodes has not been carried out yet, although the EDM performance characteristics have been studied for various materials including Ti-6Al-4V. It has been explored that type of workpiece material has the highest impact on EDM performance among the other influential factors. Thus, it is obvious that the EDM performance characteristics are not identical for all workpiece-electrode material combination. Besides, the preceding research work reveals that the effects of servo-voltage on the machining performance of EDM on titanium material (Ti-6Al-4V) has not been considered, although distinct parameters such as current, pulse-off time and duty factor has been considered. It is found that copper, aluminium and graphite has been used in machining Ti-6Al-4V; however, copper-tungsten has not been examined yet as an electrode. On the other hand, very few research works illustrate the comparative study using distinct electrode materials in surface roughness characteristics of titanium material. In this perspective, an effort has been made to study the surface characteristics namely, surface roughness ( $R_a$ ) and microstructure of the machined surface in EDM on Ti-5Al-2.5Sn titanium alloy. The microstructure of the surface is analysed for distinct discharge energies and different electrodes such as copper, copper-tungsten and graphite electrode. In this manuscript, peak current, pulse-on time, pulse-off time and servo-voltage are considered as process variables. Experiments are performed varying all these process variables for three electrode materials.

## 2 Methodology

This section is divided into three as material, process parameters and experimentation. The material section deals workpiece material and the electrodes used in this research work. Process parameters represent the input process parameters that influence the machined surface as well as the performance parameters mainly surface roughness and surface characteristics. Experimentation shows the design of experiment, experimental set-up, method of experiment and surface microstructure inspection.

### 2.1 Materials

Ti-5Al-2.5Sn titanium alloy has been selected as workpiece materials in this research. The titanium alloy Ti-5Al-2.5Sn is available commercially in many forms. The titanium alloy, Ti-5Al-2.5Sn, has excellent mechanical properties and maintains its strength at temperatures up to 600 °C [32]. The physical properties of Ti-5-2.5 alloy are listed in Table 1 [33].

**Table 1** Physical properties of titanium alloy Ti-5Al-2.5Sn

Property	Value
Density (kg/cm <sup>3</sup> )	4.48
Modulus of elasticity (GPa)	117
Specific heat capacity (J/kgK)	530
Thermal conductivity (W/mK)	7.8
Electric resistivity ( $\mu\Omega\cdot\text{m}$ )	1.6
Ultimate tensile strength (MPa)	861
Yield strength (MPa)	827
Hardness, Brinell (HB)	320
Melting temperature (°C)	1590
Beta transus temperature (°C)	1040–1090

As a fundamental requirement, the electrode material should possess high thermal conductivity, superior melting and evaporation point and the ability to be easily machined [34]. Usually, several materials—copper, graphite, copper-graphite alloys, copper-tungsten, brass, tungsten, tungsten-carbides, silver-tungsten alloy, steel, chromium and copper-chromium alloys are used as electrodes in the EDM process [35]. Copper and graphite electrodes can be used for the same EDM jobs, and these two electrodes are used extensively by the majority of EDM users in Europe, Asia and the USA [35]. On the other hand, graphite, copper, copper-tungsten, copper-graphite and brass are the most advantageous electrodes owing to their satisfactory EDM machining performance [36]. In this perspective, copper, copper-tungsten and graphite are chosen as electrode materials for the present study. The physical properties of these electrode tools are presented in Table 2 [13, 34].

### 2.2 Process parameters

Surface roughness which is the most important and frequently used parameter was chosen as the performance parameter of the EDM experiment [37]. In addition, the characteristics of surface topography of the workpiece were set as objective function in this study. Surface roughness is a measure of the texture of a surface. The surface texture is the sum of all irregularities caused by roughness, waviness and flaws. Roughness is the set of finer irregularities on the surface of a solid material, including flaws and tool marks caused by the manufacturing

**Table 2** Physical properties of copper, copper-tungsten and graphite electrodes

Properties	Material		
	Copper	Graphite	Copper-tungsten
Density (g/cm <sup>3</sup> )	8.904	1.77	15.2
Melting point (°C)	1083	3350	3500
Thermal conductivity (W/mK)	388	160–230	160

techniques used to produce the surface [38]. It is estimated by the vertical nonconformities of the actual surface (surface topography as produced and measured) from the nominal surface (intended profile of the surface topology) as shown in Fig. 1. The surface roughness can be expressed in different ways, including the arithmetic average ( $R_a$ ), root-mean-square ( $R_q$ ), average peak to valley height ( $R_z$ ) and maximum profile valley depth ( $R_{max}$ ). According to ISO 4287:1997, AA is defined as the arithmetic average roughness of the deviations of the roughness profile from the central line along the measurement [39]. Centre line average (CLA) is defined as the average value of the ordinates from the mean line, regardless of the arithmetic signs of the ordinates. The surface is rough when the deviation is large, and the surface is smooth when the deviation is small. Root-mean-square roughness ( $R_q$ ) is the square root of the average value squared, which can be expressed as in Eq. (1) [38]. Average peak to valley height (mean roughness depth) is the arithmetical mean of the single roughness depths, which can be calculated as in Eq. (2). The maximum profile valley depth ( $R_{max}$ ) is the largest of the existing single roughness depths in the total measuring length. In this study, the arithmetic average ( $R_a$ ) is used for assessment of surface roughness of the machined surface since  $R_q$  and  $R_z$  are more sensitive than  $R_a$  to changes in surface roughness.

$$R_q = \sqrt{\frac{1}{L} \int_0^L y^2(x) dx} \quad (1)$$

$$R_z = \frac{Z_1 + Z_2 + Z_3 + Z_4 + Z_5}{5} \quad (2)$$

There are a number of machining parameters, which have different effects on the EDM performance characteristics. The machining parameters and their interaction influence the EDM process performance. EDM machining parameters are divided into two groups: non-electrical parameters (injection flushing pressure and rotational speed of electrode) and electrical parameters (peak current, polarity, pulse duration and power supply voltage). However, electrical parameters are found to be more significant than non-electrical parameters in the context of machining characteristics [40]. The relevant process parameters are the peak current, pulse duration, electric polarity and properties of materials [41]. The significant parameters related to the EDM machining process are the

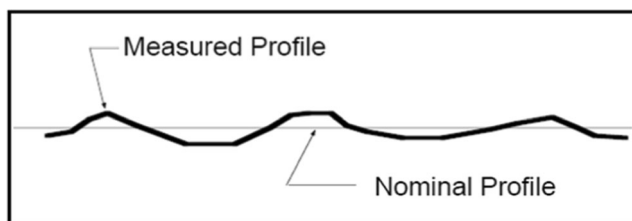


Fig. 1 Measured and nominal surface profiles

discharge current (intensity), discharge voltage, pulse-on time (pulse duration), pulse-off time (pulse interval), electrode gap (arc gap), polarity and duty cycle [42]. The parameter selection was based on the findings from a literature review and a preliminary experiment. The effects of the discharge current, voltage, pulse-on time, pulse-off time, servo-voltage, polarity, electrode material and flushing pressure were examined throughout the preliminary experiment, where the values of the distinct input parameters were varied. Abnormal discharges during machining can cause non-successive pulses such as short circuit, arcing and open circuit, indicating machining instability [43]. Therefore, the parameter ranges for normal and stable machining are set throughout the preliminary experiment. Eventually, the peak current, pulse-on time, pulse-off time, servo-voltage and tool materials were selected as the process variables for the present research. The process parameter ranges are presented in Table 3.

### 2.3 Experimentation

Careful planning of experimentation is essential in order to reduce the cost and time. The design of experiments is a powerful tool that permits analysis of the effect of process variables on response variables [44]. There are different methods for design of experiments (DOE), including factorials, fractional factorials and response surface methods. The central composite design (CCD) is more useful than full factorial designs as it requires much fewer runs to sufficiently describe the responses [14]. Thus, a number of experiments were carried out consistent with the design matrix obtained from central composite design. Experimentation was performed retaining negative polarity of the electrode. The peak current, pulse-on time, pulse-off time and servo-voltage were varied from 1 to 29 A, 10–350  $\mu$ s, 60–300  $\mu$ s and 75–115 V, respectively, during experiments. Machining was conducted on Ti-5Al-2.5Sn material using negative polarity of copper, copper-tungsten and graphite electrode stated in section 2.1. Using central composite design of response surface methods total 31 experimental set-up was obtained for selected process parameters—peak current, pulse-on time, pulse-off time and servo-voltage. Experimentation with each electrode—copper,

Table 3 The process parameters and their ranges

Process parameters	Range
Peak current (A)	1–29
Pulse-on time ( $\mu$ s)	10–350
Pulse-off time ( $\mu$ s)	60–300
Servo-voltage (V)	75–115
Polarity	negative
Electrode material	copper, copper-tungsten and graphite

copper-tungsten and graphite—was performed according to this set-up. Each experiment was carried out three times and the average value of the surface roughness was considered for analysis surface finish characteristics. The value of arithmetic average surface roughness ( $R_a$ ) was assessed using the Perthometer S2 from Mahr, Germany. In measuring the roughness of the machined surface, five observations were done on different positions of the machined surface for each sample. The average of these five assessments was considered as the value of surface roughness,  $R_a$ .

Surface texture analysis was carried out by scanning electronic microscopy to observe the surface topography of selected specimens. The experiments mainly varied the energy intensity ( $I_p \times T_{on}$ ) for a specific electrode, since the surface attribute is mainly associated with pulse energy (pulse current and/or pulse-on time) as shown in Table 4 [45]. The specimens were got ready after experiments. During the experiment, the value of pulse-off time and servo-voltage were set as 120  $\mu$ s and 85 V respectively. Then, the microstructure of the workpiece surface was investigated using SEM model-EVO 50 from Zeiss, Germany. All specimens were analysed with regard to all three electrode materials, namely copper, copper-tungsten and graphite. SEM micrographs are accomplished from the machined surface at 500 $\times$  magnification size. The surface characteristics are investigated for distinct discharge energies, as well as the SEM micrographs are analysed considering all electrodes collectively to explore the effect of the electrode.

### 3 Results and discussion

The obtained data are analysed and studied accomplishing the experimental work as design of experiment stated above. The analysed results are shown in Section 3.1. In the same section, the results are also explained well following the observation. The surface microstructure was investigated using scanning electronic microscopy (SEM) as stated in methodology. The investigations against different electrodes—copper, copper-tungsten and graphite and diverse energies—are demonstrated in Section 3.2. The acquired microstructures in distinct circumstances are discussed too in the same part. The effects of electrode on the surface topography are shown in Section 3.3.

**Table 4** Set of designed experiments for SEM viewing

Sl no.	Peak current (A)	Pulse-on time ( $\mu$ s)
1	15	180
2	29	320
3	2	95

### 3.1 Effect of electrical parameters on surface roughness

The effect of each of the process parameters—peak current, pulse-on time, pulse-off time and servo-voltage—on the surface roughness is illustrated in this section considering negative polarity of the electrode. This is studied by varying one input parameter between its minimum and maximum value while the other input parameters are retained fixed in their reference condition. The reference condition is the mean value of the parameter.

The impact of the peak current on the surface roughness is shown in Fig. 2. Figure 2 also depicts the impacts of the electrode on the workpiece surface roughness for copper, copper-tungsten and graphite electrode. It is apparent from Fig. 2 that the surface roughness increases gradually with increasing peak current. The crater size increases with an increase of current. Besides, as pulse current increases, discharges strike the surfaces more intensely, hence a great quantity of molten and floating metal is suspended in the electrical discharge gap during EDM [27]. Ultimately, the surface finish becomes rougher with the increase of peak current [46]. On the other hand, low discharge current creates small craters leading to a smooth surface finish [47]. Thus, the surface roughness of the machined surface rises with an increase of peak current, and a lower surface roughness is achieved at low ampere. A similar observation was reported in prior study [48].

Fig. 2 exhibits that the surface roughness increases as the peak current increases for all three electrodes. The results indicate that the lowest surface roughness is achieved with a copper electrode compared with the copper and graphite electrodes. On the other hand, the graphite electrode gives the highest surface roughness among the three electrode materials. Lee and Li [49] reported that copper-tungsten electrodes provide better surface finish compared to graphite electrodes in EDM on tungsten

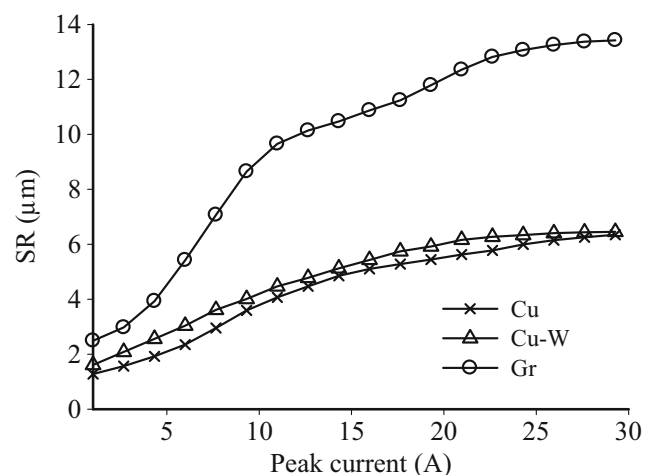


**Fig. 2** Surface roughness for varied peak current

carbide. They also found that the copper tool gives the best surface attributes, while graphite gives the poorest surface.

The effect of pulse-on time and the impact of the electrode material on the workpiece surface roughness are presented in Fig. 3. It is apparent from this figure that the surface roughness increases upon increasing the pulse-on time. However, it is seen that initially the surface roughness increases until a specific (peak) value and then does not vary significantly when the pulse-on time increases for copper electrode. On the other hand, after the peak value of SR, the surface roughness tends to decrease as the pulse-on time increases for copper-tungsten electrodes.

The crater formation and material erosion are proportional to the amount of applied energy during on-time, which is a function of discharge current and pulse-on time. This discharge energy is directly related to the pulse-on time [47]; therefore, a long pulse-on time creates more craters and erodes more material [50]. As a consequence, a long pulse-on time generates a rougher surface. The low surface roughness of the EDM machined surface is achieved at low pulse-on time. During the EDM process, various sizes of discharge craters are generated on the machined surface due to melting, vaporization and the impulsive force of dielectric explosion, so the topography of the machined surface is irregular [51]. The energy density is reduced within the discharge spot upon extending the pulse-on time, and a tenuous discharge occurs as a result [52, 49]. The amount of workpiece material removed at a single pulse is reduced, and the surface topography becomes more even [51]. Thus, the surface roughness tends to decline under longer pulse duration.

The effect of pulse-off time and the impact of the electrode material on surface roughness are shown in Fig. 4. This figure shows the diverse effect of the pulse-off time on surface roughness characteristics. As can be seen from the figure, an increase in pulse-off time initially increases surface roughness until the peak value of surface roughness then reduces the

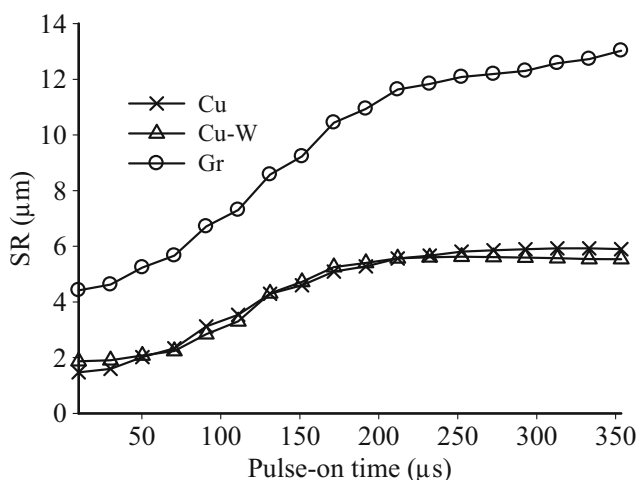


Fig. 3 Surface roughness for varied pulse-on time

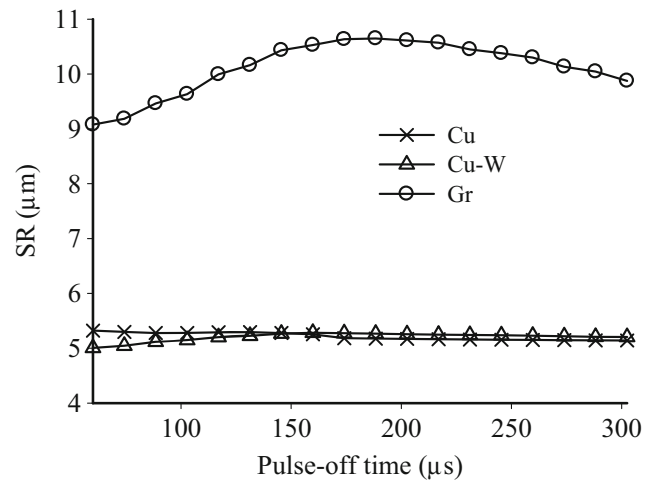


Fig. 4 Surface roughness for varied pulse-off time

surface roughness. On the other hand, a falling tendency of the surface roughness graph is observed as pulse-off time is increased for copper electrode. If the pulse-off time is too short, there is not enough time to clear the disintegrated particles from the gap between the electrode and the workpiece [49]. The too short pulse-off time induces an unstable spark discharge because of insufficient insulation recovery [53]. Then again, a long pulse-off time influences the cooling effect on the electrode and workpiece surface, and more energy is required to establish the plasma channel; consequently, there is higher surface roughness. Accordingly, it is obvious that the pulse-off time must be sufficiently long to acquire a uniform erosion of material from the surface of the workpiece and stable machining process; otherwise, a non-uniform erosion of the workpiece surface will occur. Thus, the surface roughness tends to decrease after certain value of pulse-off time.

The effect of the servo-voltage on the surface roughness is shown in Fig. 5. Figure 5 also depicts the effect of the electrode on the surface roughness for copper, copper-tungsten and graphite electrode. It is apparent from Fig. 5 that as the

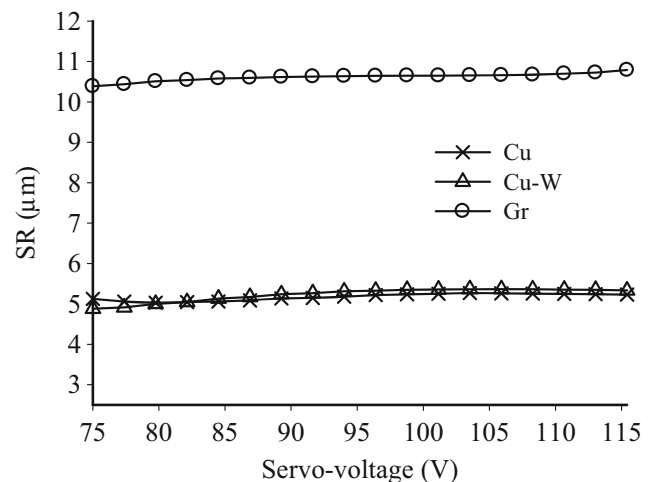


Fig. 5 Surface roughness for varied servo-voltage

servo-voltage increases the surface roughness tends to increase. The servo-voltage controls the spark gap during the process of EDM, and the spark gap increases as the servo-voltage increases. At the high servo-voltage, the electrode is not able to advance longer towards the workpiece. Therefore, the material erosion as well as the surface roughness supposed to be decreased whilst the servo-voltage increases. On the contrary, here, the surface roughness increases with servo-voltage due to the negative polarity of the electrode and unstable machining. An extended discharge waveform is found at the pulse-off time when the polarity is negative. This is because many particles of copper and tungsten electrodes drop and accumulate to the machined surfaces, interfering with the discharge proceeding. Accordingly, the discharge state becomes rather unstable. Thus, the machining causes higher surface roughness. It is apparent that the surface roughness is significantly influenced by the peak current and pulse-on time among the selected parameters (peak current, pulse-on time, pulse-off time and servo-voltage).

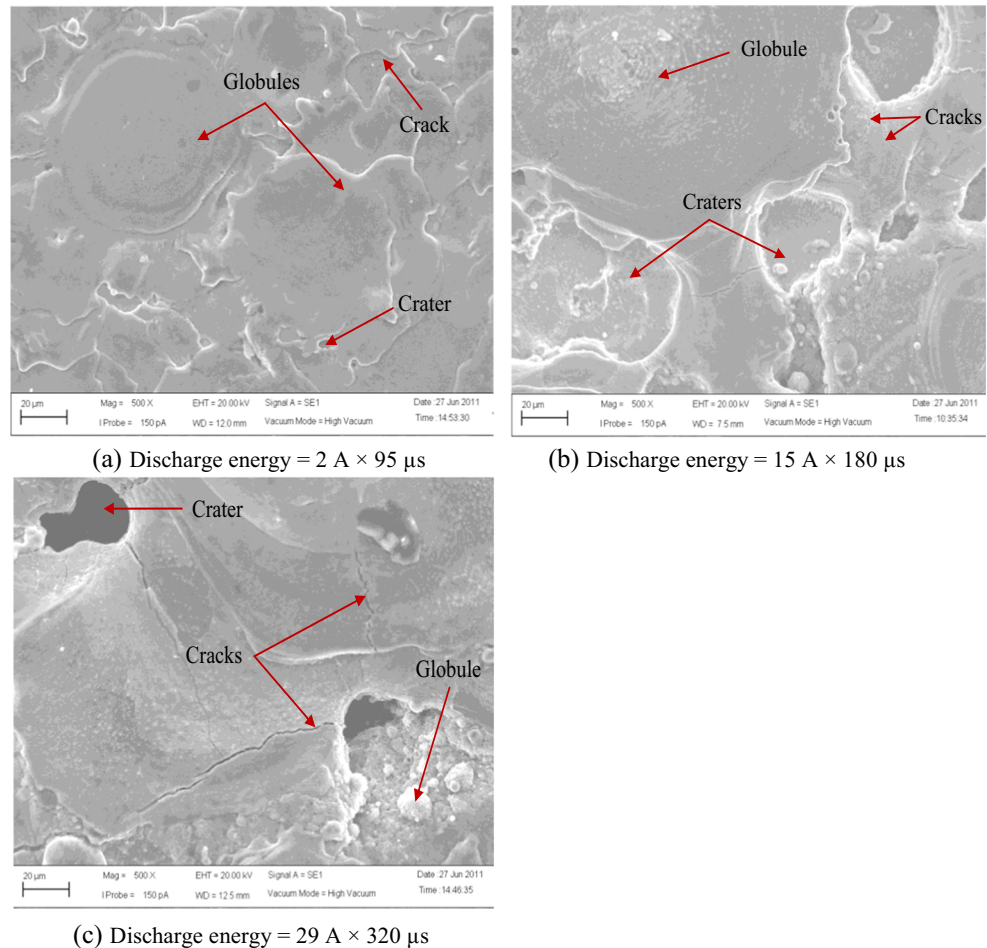
It is seemed that the machining with copper electrode produces the lowest surface roughness; however, the surface roughness with copper and copper-tungsten electrodes is nearly similar. On the other hand, the graphite

produces, on average, approximately double surface roughness than that for copper-tungsten electrode. Hascalik and Caydas [13] noticed that the graphite electrode leads to a considerable increase in surface roughness. The thermo-physical properties of the electrode material significantly regulate the performance characteristics of EDM. The thermo-physical properties of graphite are very different from other electrodes—copper and copper-tungsten [35]. Accordingly, the graphite electrode facilitates more stable machining than copper, which produces a poor surface. EDM with graphite causes more erosion of graphite electrode since the graphite possesses high porosity compared to copper and copper-tungsten electrodes. Thus, the graphite electrode yields highest surface roughness.

### 3.2 Microstructure of the machined surface

The surface topography of a number of samples is investigated using scanning electronic microscopy to analyse the surface characteristics of the machined surface. The analysis is performed for different electrodes (copper, copper-tungsten and graphite) separately. The surface characteristics are

**Fig. 6** Surface topography of the machined surface with Cu electrode



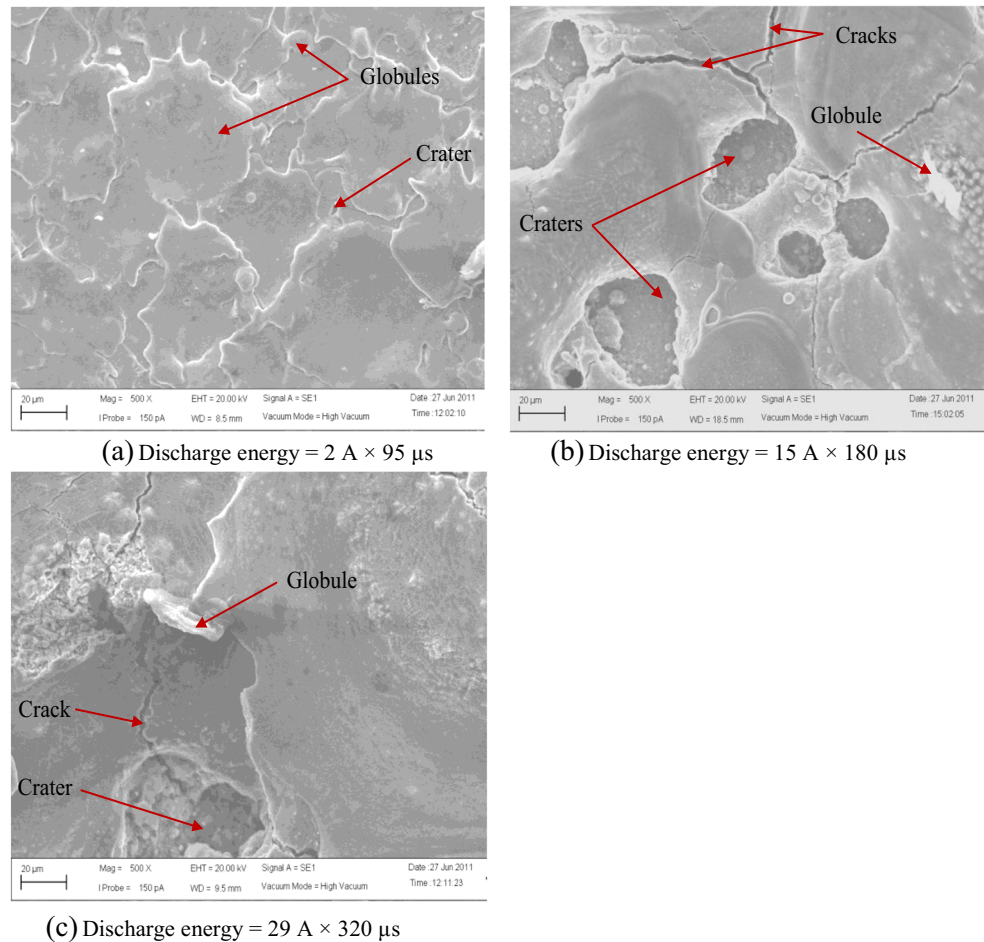
investigated for distinct discharge energy ( $2 \text{ A} \times 95 \text{ } \mu\text{s}$ ,  $15 \text{ A} \times 180 \text{ } \mu\text{s}$  and  $29 \text{ A} \times 320 \text{ } \mu\text{s}$ ).

### 3.2.1 Copper electrode

Figure 6 shows the surface topography of the specimen machined with a copper electrode for distinct discharge energy. Scanning electronic microscopic views reveal shallow craters, a few microcracks and globules of debris on the surface, as shown in Fig. 6a. The surface topography looks like liquid metal that has been poured and resolidified, creating a layer as shown in Fig. 6a. The surface contains very few craters; however, most of the surface is covered with globules. The microcracks initiated at the recast layer penetrate towards the parental material perpendicular to the machined surface. The thermal energy obtained from a series of successive sparks generates high-temperature plasma and erodes material from the workpiece. The spark occurring through the high-temperature plasma melts and vaporizes a small area of the workpiece surface, and ultimately, craters are formed. The crater size depends on the pulse current as well as the discharge energy, and low discharge energy produces small crater [54].

SEM depicts the presence of microcracks resulting from rapid cooling of the recast layer. The crack propagation through the brittle recast layer is fairly fast and continues more slowly into the tougher (bulk) material. Many surface imperfections in the recast layer produced by the EDM process initiate cracking. The cracks are in the form of microcracks. On the other hand, cracks are not readily formed within a thin recast layer because it is able to dissipate heat rapidly [55]. Therefore, lower discharge energy produces microcracks. A similar observation was reported for electrical discharge machining on M2 die steel [56]. At the end of pulse-on time, a small amount of molten material is not expelled; although, most of the melted and vaporized material is flushed away by the dielectric [57]. Since the flushing cannot eject all of the molten materials, a portion of the melted electrode accumulates on the workpiece surface, producing globules of debris. Thus, low discharge energy creates small and shallow craters, microcracks and globules. Some of these are very small and attached to the surface, appearing like pockmarks. A layer containing numerous pock marks, globules, craters, microcracks and cracks is visible on the machined surface. This layer is called the recast layer, and the density and size of features of the recast layer depend on machining conditions.

**Fig. 7** Surface topography of the machined surface with Cu-W electrode



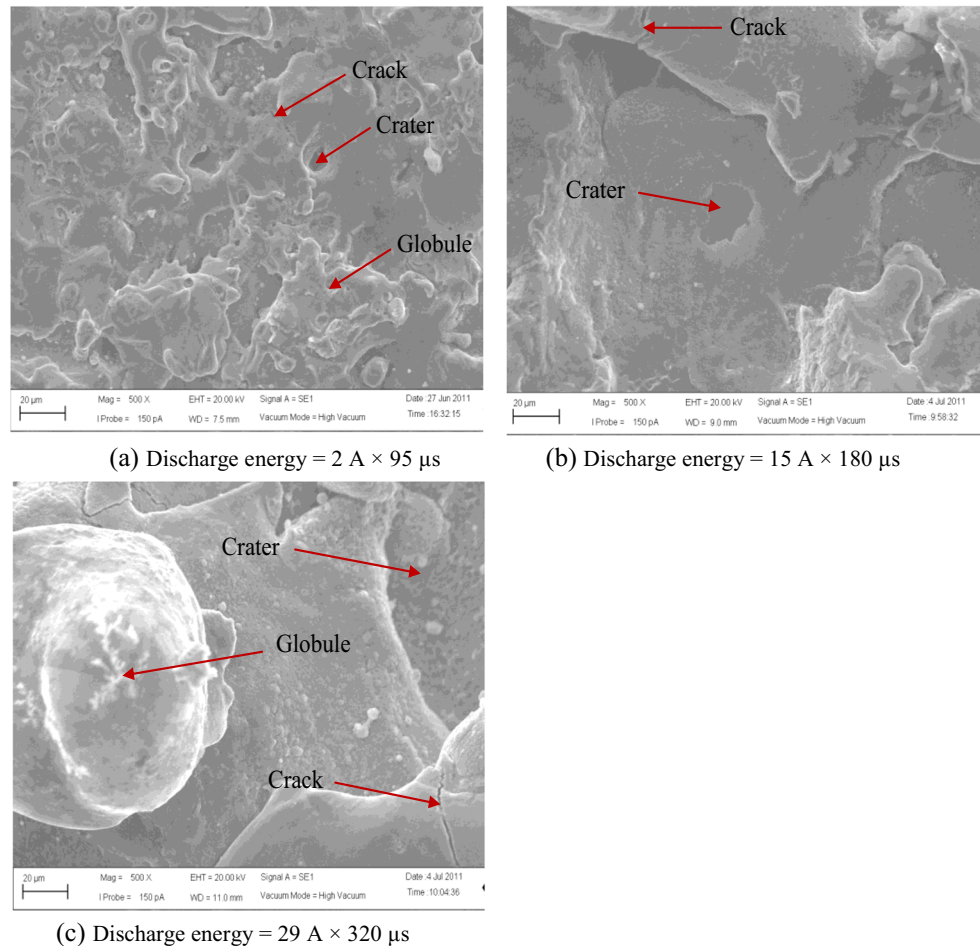
According to the SEM image in Fig. 6, the surface characteristics (crater, crack and globule) are distorted on account of discharge energy. The size and depth of the discharge craters increase as the discharge energy level increases. The increase of discharge current and pulse-on time increases the discharge energy. The large discharge energy causes violent sparks and impulsive force, which strike the surface. The large impulsive force advances in the spark gap. The rate of melting and vaporization is increased, resulting in a greater material removal rate [27]. This results in larger and deeper craters on the machined surface [58]. The long pulse-on time is responsible for larger craters; however, strong peak current causes deep craters at high discharge energy. Therefore, high discharge energy produces deeper and wider craters, generating a rougher surface. The globule formation depends on the erosion of the electrode, which in turn depends on the discharge energy. The high discharge energy produces an inhibitor carbon layer on the electrode surface [59]. The amount of carbon accumulated on the electrode surface increases considerably according to the increase of pulse-on time. This carbon layer reduces the electrode wear [12]. Again, the resolidified particles are ejected from the gap between the electrode and the workpiece by dielectric flushing and impulsive force [49, 60]. The high

discharge energy causes a large impulsive force, which can remove more debris from the machining gap [60]. Thus, the surface topography with high discharge energy presents a smaller number of globules and pock marks.

### 3.2.2 Copper-tungsten electrode

The surface topography of the machined surface with a Cu-W electrode is presented in Fig. 7 for distinct discharge energy. Craters, globules of debris, cracks and pockmarks are found in the surface structure. The spark occurred during discharge melts and vaporizes the material from the workpiece surface. As a consequence, numerous minute craters are formed in the surface [51]. The molten material is not flushed out completely owing to inadequate flushing through the micro-gap between the electrode and workpiece [57]. Therefore, the remaining molten material is cooled rapidly and resolidified on the surface. The rapid cooling of the recast layer causes residual stresses in the machined surface. When the residual stresses exceed the ultimate tensile strength of the base material, cracks are formed in the surface [61]. The size of the craters and the degree of cracking increase as discharge energy increases as shown in Fig. 7.

**Fig. 8** Surface topography of the machined surface with Gr electrode



A high discharge energy increases the rate of melting and vaporization, which causes larger and deeper craters [27]. Generally, the diameter and the depth of craters increase with an increase in peak current [58]. On the other hand, the high discharge energy results in a thick recast layer as well as increased residual stress at the machined surface [45]. The number and size of cracks increases with pulse-on time. Thus, larger and deeper craters and a greater degree of cracking are evident at higher discharge energy. It is interesting to note that a lower discharge energy level ( $15 \text{ A} \times 180 \mu\text{s}$ ) carries smaller craters in combination with a higher degree of cracking, as shown in Fig. 7b. In contrast, a higher discharge energy level ( $29 \text{ A} \times 320 \mu\text{s}$ ) produces larger craters together with a lower degree of cracking, as shown in Fig. 7c. Lee and Tai [55] observed larger crack widths for small peak current. It is evident that the number of craters and the volume of material removed are directly related to the discharge energy [49]. When the discharge energy is high, the amount of material erosion is increased, creating more craters. Similarly, lower

discharge energy reduces the amount of material erosion, resulting smaller craters. Then again, the formation of enlarged craters and more globules causes a wide variation in the thickness of the white layer (Fig. 7c). Moreover, no significant increase in the induced stress is apparent at high peak current, signifying a lower degree of cracking as Fig. 7c [55]. Thus, a higher degree of cracking and small craters are apparent in Fig. 7b, and the opposite can be seen in Fig. 7c.

### 3.2.3 Graphite electrode

The surface topography of the machined surface generated during EDM with a graphite electrode is shown in Fig. 8 for distinct discharge energy. The machined surface is characterized by globules, craters, cracks and small debris (like pock-marks) as the surface obtained with other two electrodes (copper and copper-tungsten). The reason for the formation of craters, globules and cracks has been discussed above. It is seen that the amount of craters, crack and globules are

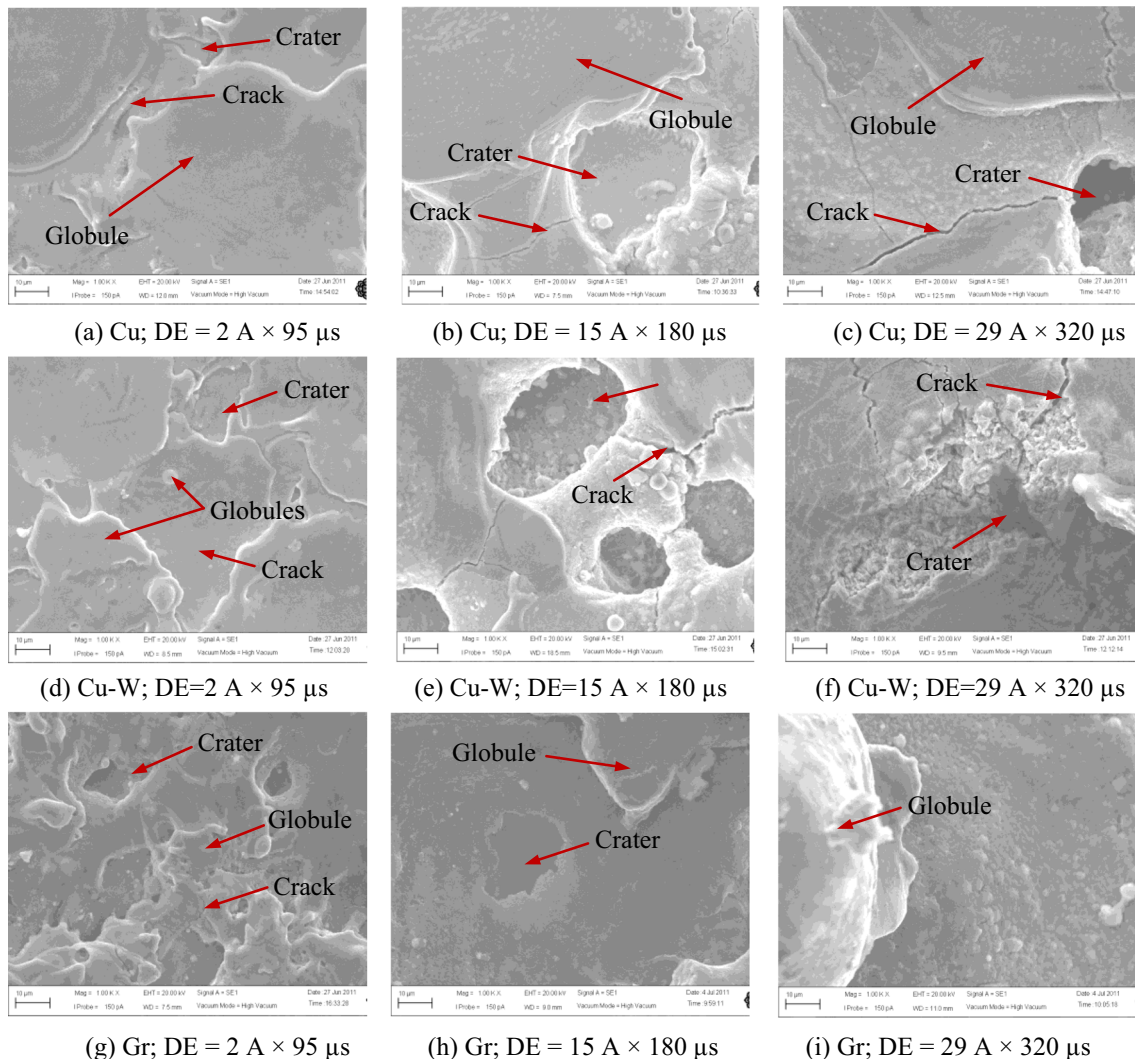


**Fig. 9** Surface topography of the machined surface with different electrodes for altered discharge energy

increased when the discharge energy is increased, as shown in Fig. 8a–c. At high discharge energy, since there is a high rate of erosion of the material which produces larger craters. Furthermore, there is high impulsive force, which increases the yield stress of the surface. As a consequence, high discharge energy produces a higher degree of cracking. Thus, the surface finish obtained at high discharge energy yields more craters and globules, resulting in a poor surface, and it has been discussed before.

### 3.3 Effect of electrode on microstructure

The formation of craters, cracks and globules on the machined surface of the workpiece in machining with copper, copper-tungsten and graphite electrodes has been demonstrated separately in the previous section. Besides, the amount and size of these features have been illustrated for different electrodes and altered discharge energy. The SEM micrographs of the machined surfaces are presented in Fig. 9 to compare the surface topography among different electrodes with a negative polarity condition.

In this figure, it is observed that the surface obtained using copper electrode yields greater amount of globules along with small craters and cracks. The more tool wear is occurred when EDM with copper electrode as compared to copper-tungsten electrode. A part of the molten material of the electrode is dropped on the workpiece surface creating globules due to inadequate flushing. Therefore, more globules are generated while machining with copper electrode. However, the copper-tungsten electrode causes larger crater and higher degree of crack comparing with copper electrode. Copper-tungsten electrode concentrates greater amount of heat rather than dissipation because of its low thermal conductivity [34]. As a result, the intensity of heat energy increases, which erodes more material from the workpiece. Thus, the copper-tungsten produces larger crater and higher degree of crack deteriorating the surface finish. Graphite electrode produces largest size of craters among these three electrodes. The negative graphite electrode provides high material removal as compared with other electrode [13]. Accordingly, it generates greatest amount of craters resulting larger size of craters.

The copper electrode provides smallest craters, cracks of lower degree in combination with more globules. On the other hand, largest craters appeared in the topography of the machined surface applying negative graphite electrode followed by copper-tungsten electrode. Thus, it can be understood that the copper electrode produces the finest surface structure whilst graphite delivers worst surface characteristics. In consequence, the copper can become as first choice electrode materials for Ti-5Al-2.5Sn titanium alloy material.

## 4 Conclusion

An extensive analysis has been conducted to investigate the effect of machining parameters namely, peak current, pulse-on time, pulse-off time, servo-voltage and electrode materials on surface roughness and surface structure in EDM of Ti-5Al-2.5Sn titanium alloy. The following conclusions can be drawn in this research work.

The surface roughness of the machined surface increases upon increasing the peak current, pulse-on time and servo-voltage. A lower surface roughness is achieved at low ampere. Again, the surface roughness increases until a specific value and then does not vary significantly when the pulse-on time increases for copper electrode. For copper-tungsten electrodes, the surface roughness tends to decrease after its peak value as the pulse-on time increases. The pulse-off time affects the surface roughness diversely. The pulse-off time must be sufficiently long to acquire a uniform erosion of material from the surface of the workpiece and stable machining process. The surface roughness is greatly influenced by peak current and pulse-on time among the selected electrical parameters.

The copper electrode produces the lowest surface roughness and graphite electrode gives the highest surface roughness among the three electrode materials. However, the surface roughness with copper and copper-tungsten electrodes is nearly alike. The graphite electrode produces, on average, approximately double surface roughness than that of copper-tungsten electrode. Among the three electrodes, copper electrode can be used whilst fine surface is required.

EDM process produces surface topography with craters, cracks and globules of debris. The size of the craters and the degree of cracking increase as discharge energy increases. Low discharge energy produces small crater and high discharge energy produces deeper and wider craters generating a rougher surface.

The surface obtained using copper electrode yields greater amount of globules along with small craters and cracks. The copper-tungsten electrode causes larger crater and higher degree of crack as compared to copper electrode. The largest craters appeared in the topography of the machined surface applying graphite electrode followed by copper-tungsten electrode. The copper electrode produces the finest surface structure whilst graphite delivers worst surface characteristics. In context of fine surface characteristics, the copper can become as first choice electrode materials for Ti-5Al-2.5Sn titanium alloy material.

Further work can be carried out in order to investigate the effect of process parameters on tool wear and machining speed. The optimum value of the performance characteristic parameters as well as the multi-objective optimization could be set-up. On the other hand, the research work will be carried on considering positive polarity along with the comparison

between negative and positive polarity. Future work insists the attention in view of gap voltage and duty factor input process parameters for machining characteristics.

**Acknowledgments** The authors would like to acknowledge the support of the Universiti Malaysia Pahang (UMP) for Doctoral Scholarship Scheme. The sincere thanks of the authors go to the Faculty of Mechanical Engineering, UMP, for providing the lab facilities. Besides, the author would like to express their earnest gratitude to the authority of Noakhali Science and Technology University (NSTU), Noakhali, Bangladesh, for their support.

## References

- Liu X, Chu PK, Din C (2004) Surface modification of titanium, titanium alloys, and related materials for biomedical applications. *Mater Sci Eng R*. doi:10.1016/j.mser.2004.11.001
- Kuroda D, Niinomi M, Morinaga M, Kato Y, Yashiro T (1998) Design and mechanical properties of new  $\beta$  type titanium alloys for implant materials. *Mater Sci Eng A*. doi:10.1016/S0921-5093(97)00808-3
- Khan MAR, Rahman MM, Kadirgama K (2015) An experimental investigation on surface finish in die-sinking EDM of Ti-5Al-2.5Sn. *Int J Adv Manuf Technol*. doi:10.1007/s00170-014-6507-y
- Rahman MM, Khan MAR, Kadirgama K, Noor MM, Bakar RA (2010). Mathematical modeling of material removal rate for Ti-5Al-2.5Sn through EDM process: a surface response method. *Advances in Control, Chemical Engineering, Civil Engineering and Mechanical Engineering* 34–37
- Khan MAR, Rahman MM, Kadirgama K, Ismail AR (2012a) Mathematical model for wear rate of negative graphite electrode in electrical discharge machining on Ti-5Al-2.5Sn. *Jurnal Teknologi* 59:57–61
- Lovatt R (2008) The development of a lightweight electric vehicle chassis and investigation into the suitability of tial for automotive applications. M.Sc. Thesis. The University of Waikato, Hamilton, New Zealand
- Khan MAR, Rahman MM, Kadirgama K, Maleque MA, Bakar RA (2011a) Artificial intelligence model to predict surface roughness of Ti-15-3 alloy in EDM process. *World Academic Science Engineering Technology* 74:121–125
- Rahman MM, Khan MAR, Noor MM, Kadirgama K, Bakar RA (2011) Optimization of machining parameters on surface roughness in EDM of Ti-6Al-4V using response surface method. *Advance Materials Research*. doi:10.4028/www.scientific.net/AMR.213.402
- Khan MAR, Rahman MM, Kadirgama K (2012b) Mathematical model and optimization of surface roughness during electrical discharge machining of Ti-5Al-2.5Sn with graphite electrode. *Adv Sci Lett*. doi:10.1166/asl.2012.4211
- Khan MAR, Rahman MM, Kadirgama K, Bakar RA (2012c) Artificial neural network model for material removal rate of Ti-15-3 in electrical discharge machining. *Energy Education Science and Technology Part A: Energy Science and Research* 29(2):1025–1038
- Maher I, Ling LH, Sarhan AAD, Hamdi M (2015) Improve wire EDM performance at different machining parameters—ANFIS modelling. *IFAC-PapersOnLine* 48(1):105–110
- Chen SL, Yan BH, Huang FY (1999) Influence of kerosene and distilled water as dielectrics on the electric discharge machining characteristics of Ti-6Al-4V. *Journal of Materials Processing Technologies* 87:107–111
- Hascalik A, Caydas U (2007) Electrical discharge machining of titanium alloy (Ti-6Al-4V). *Appl Surf Sci*. doi:10.1016/j.apsusc.2007.05.031
- Caydas U, Hascalik A (2008) Modeling and analysis of electrode wear and white layer thickness in die-sinking EDM process through response surface methodology. *International J Adv Manuf Technol*. doi:10.1007/s00170-007-1162-1
- Fonda P, Wang Z, Yamazaki K, Akutsu Y (2008) A fundamental study on Ti-6Al-4V's thermal and electrical properties and their relation to EDM productivity. *Journal of Materials Processing Technologies*. doi:10.1016/j.jmatprotec.2007.09.060
- Rao GKM, Janardhana GR, Rao DH, Rao MS (2008) Development of hybrid model and optimization of metal removal rate in electric discharge machining using artificial neural networks and genetic algorithm. *ARPN Journal of Engineering and Applied Science* 3(1):19–30
- Rao GKM, Rangajanardhaa G, Rao DH, Rao MS (2009) Development of hybrid model and optimization of surface roughness in electric discharge machining using artificial neural networks and genetic algorithm. *Journal of Materials Processing Technologies*. doi:10.1016/j.jmatprotec.2008.04.003
- Kao JY, Tsao CC, Wang SS, Hsu CY (2010) Optimization of the EDM parameters on machining Ti-6Al-4 V with multiple quality characteristics. *Int J Adv Manuf Technol*. doi:10.1007/s00170-009-2208-3
- Raghav G, Kadam BS, Kumar M (2013) Optimization of material removal rate in electric discharge machining using mild steel. *International Journal of Emerging Science and Engineering* 1(7): 2319–6378
- Pawade MM, Banwait SS (2013) A brief review of die sinking electrical discharging machining process towards automation. *Am J Mech Eng*. doi:10.12691/ajme-1-2-4
- Khan MAR, Rahman MM (2013) Development of regression equation for surface finish and analysis of surface integrity in EDM. *International Journal of Mechanical, Industrial Science and Engineering* 7(3):105–110
- Ahmad S, Lajis MA (2013) Electrical discharge machining (EDM) of inconel 718 by using copper electrode at higher peak current and pulse duration. *IOP Conf Series : Materials Science and Engineering* 50:1–7
- Daneshmand S, Kahrizi EF, Abedi E, Abdolhosseini MM (2013) Influence of machining parameters on electro discharge machining of niti shape memory alloys. *Int J Electrochem Sci* 8:3095–3104
- Gill AS, Kumar S (2016) Surface roughness and microhardness evaluation for EDM with Cu-Mn powder metallurgy tool. *Journal of Materials and Manufacturing Processes* 31(4):514–521. doi:10.1080/10426914.2015.1070412
- Gopalakannan S, Senthilvelan T (2012) Effect of electrode materials on electric discharge machining of 316 L and 17-4 PH stainless steels. *J Miner Mater Charact Eng* 11:685–690
- Hegab HA, Gadallah MH, Esawi AK (2015) Modeling and optimization of electrical discharge machining (EDM) using statistical design. *Manuf Rev*. doi:10.1051/mfreview/2015023
- Kathiresan M, Somakumar T (2010) EDM studies on aluminum alloy-silicon carbide composites developed by vortex technique and pressure die casting. *Journal of Minerals & Materials Characterization & Engineering* 9(1):79–88
- Reddy VV, Valli PM, Kumar A, Reddy CS (2015) Influence of process parameters on characteristics of electrical discharge machining of PH17-4 stainless steel. *J Adv Manuf Syst*. doi:10.1142/S0219686715500122
- Singh B, Singh P, Tejpal G, Singh G (2012) An experimental study of surface roughness of h11 steel in EDM process using copper tool electrode. *International Journal of Advanced Engineering Technology* 3(4):130–133

30. Daneshmand S, Kahrizi EF, Neyestanak AAL, Monfared V (2014) Optimization of electrical discharge machining parameters for Niti shape memory alloy by using the Taguchi method. *J Mar Sci Technol*. doi:10.6119/JMST-013-0624-1
31. Gostimirovic M, Kovac P, Sekulic M, Skoric B (2012) Influence of discharge energy on machining characteristics in EDM. *J Mech Sci Technol*. doi:10.1007/s12206-011-0922-x
32. Kopeliovich D (2009) Titanium alpha and near alpha alloys. *Substances and Technologies*. [http://www.substech.com/dokuwiki/doku.php?id=titanium\\_alpha\\_and\\_near-alpha\\_alloys](http://www.substech.com/dokuwiki/doku.php?id=titanium_alpha_and_near-alpha_alloys). Accessed 28 Feb 2009
33. Kopeliovich D (2008) Titanium alpha alloy, grade 6 (Ti-5Al-2.5Sn). *Substances and Technologies*. [http://www.substech.com/dokuwiki/doku.php?id=titanium\\_alpha\\_alloy\\_grade\\_6\\_ti-5Al-2.5Sn](http://www.substech.com/dokuwiki/doku.php?id=titanium_alpha_alloy_grade_6_ti-5Al-2.5Sn). Accessed 16 May 2008
34. Jahan MP, Wong YS, Rahman M (2009) A study on the fine-finish die-sinking micro-EDM of tungsten carbide using different electrode materials. *J Mater Process Technol*. doi:10.1016/j.jmatprotec.2008.09.015
35. Amorim FL, Weingaertner WL (2007) The behavior of graphite and copper electrodes on the finish die-sinking electrical discharge machining (EDM) of AISI P20 tool steel. *J Braz Soc Mech Sci Eng* 29(4):367–371
36. Mehta S, Rajurkar A, Chauhan J (2009) A review on current research trends in die-sinking electrical discharge machining of conductive ceramics. *International Journal of Recent Trends in Engineering* 1(5):100–104
37. Khan MAR, Rahman MM, Kadirgama K, Maleque MA, Ishak M (2011b) Prediction of surface roughness of Ti-6Al-4V in electrical discharge machining: a regression model. *Journal of Mechanical Engineering and Science* 1:16–24
38. Jones FD, Ryffel HH, Oberg E, McCauley CJ, Heald RM (2004) *Machinery's handbook*, 27th edn. Industrial Press, New York, pp 629–745
39. Wu KL, Yan BH, Huang FY, Chen SC (2005) Improvement of surface finish on SKD steel using electro-discharge machining with aluminum and surfactant added dielectric. *International Journal of Machine Tools & Manufacture*. doi:10.1016/j.ijmachtools.2004.12.005
40. Abu Zeid OA (1997) On the effect of electrodischarge machining parameters on the fatigue life of AISI D6 tool steel. *Journal of Materials Processing Technologies* 68:27–32
41. Tsai KM, Wang PJ (2001) Semi-empirical model of surface finish on electrical discharge machining. *International Journal of Machine Tools & Manufacture* 41:1455–1477
42. Garg RK, Singh KK, Sachdeva A, Sharma VS, Ojha K, Singh S (2010) Review of research work in sinking EDM and WEDM on metal matrix composite materials. *Int J Adv Manuf Technol*. doi:10.1007/s00170-010-2534-5
43. Mahdavejad RA (2009) EDM process optimisation via predicting a controller model. *Archives of Computational Materials Science and Surface Engineering* 1(3):161–167
44. Puertas I, Luis CJ (2003) A study on the machining parameters optimisation of electrical discharge machining. *Journal of Materials Processing Technologies*. doi:10.1016/S0924-0136(03)00392-3
45. Ramasawmy H, Blunt L, Rajurkar KP (2005) Investigation of the relationship between the white layer thickness and 3D surface texture parameters in the die-sinking EDM process. *Precis Eng*. doi:10.1016/j.precisioneng.2005.02.001
46. Soni JS, Chakraverti G (1995) Effect of electrode material properties on surface roughness and dimensional accuracy in electro-discharge machining of high carbon high chromium die steel. *Journal of institution engineering (India) Part PR: Production Engineering Division* 76:46–51
47. Pradhan MK, Biswas CK (2009) Modeling and analysis of process parameters on surface roughness in EDM of AISI D2 tool steel by RSM approach. *International Journal of Engineering and Applied Sciences* 5(5):346–351
48. Amorim FL, Weingaertner WL (2004) Die-sinking electrical discharge machining of a high-strength copper-based alloy for injection molds. *J Braz Soc Mech Sci Eng* 26(2):137–144
49. Lee SH, Li XP (2001) Study of the effect of machining parameters on the machining characteristics in electrical discharge machining of tungsten carbide. *Journal of Materials Processing Technologies* 115:344–358
50. Ramasawmy H, Blunt L (2004) Effect of EDM process parameters on 3D surface topography. *Journal of Materials Processing Technologies*. doi:10.1016/S0924-0136(03)00652-6
51. Lin YC, Lee HS (2008) Machining characteristics of magnetic force-assisted EDM. *Int J Mach Tools Manuf*. doi:10.1016/j.ijmachtools.2008.04.004
52. Kiyak M, Cakir O (2007) Examination of machining parameters on surface roughness in EDM of tool steel. *J Mater Process Technol*. doi:10.1016/j.jmatprotec.2007.03.008
53. Wu KL, Yan BH, Lee JW, Ding CG (2009) Study on the characteristics of electrical discharge machining using dielectric with surfactant. *Journal of Materials Processing Technologies*. doi:10.1016/j.jmatprotec.2008.09.005
54. Descoedres, A. (2006). *Characterization of electrical discharge machining plasmas*. Ph.D. Thesis. Ecole Polytechnique Federale de Lausanne, Switzerland
55. Lee HT, Tai TY (2003) Relationship between EDM parameters and surface crack formation. *J Mater Process Technol*. doi:10.1016/S0924-0136(03)00688-5
56. Bhattacharyya B, Gangopadhyay S, Sarkar BR (2007) Modelling and analysis of EDMED job surface integrity. *J Mater Process Technol*. doi:10.1016/j.jmatprotec.2007.01.018
57. Bonny K, Baets PD, Wittenberghe JV, Delgado YP, Vleugels J, Biest OV et al (2010) Influence of electrical discharge machining on sliding friction and wear of WC–Ni cemented carbide. *Tribol Int*. doi:10.1016/j.triboint.2010.08.008
58. Chiang KT (2008) Modeling and analysis of the effects of machining parameters on the performance characteristics in the EDM process of Al<sub>2</sub>O<sub>3</sub>+TiC mixed ceramic. *Int J Adv Manuf Technol*. doi:10.1007/s00170-007-1002-3
59. Yan BH, Lin YC, Huang FY, Wang CH (2001) Surface modification of SKD 61 during EDM with metal powder in the dielectric. *Materials Transaction JIM* 42(12):2597–2604
60. Patel KM, Pandey PM, Rao PV (2009) Determination of an optimum parametric combination using a surface roughness prediction model for EDM of Al<sub>2</sub>O<sub>3</sub>/SiCw/TiC ceramic composite. *Mater Manuf Process*. doi:10.1080/10426910902769319
61. Senthilkumar V, Omprakash BU (2011) Effect of titanium carbide particle addition in the aluminium composite on EDM process parameters. *Journal of Manufacturing Process*. doi:10.1016/j.jmapro.2010.10.005